Metallic glass formation in highly undercooled $Zr_{41.2}Ti_{13.8}Cu_{12.5}Ni_{10.0}Be_{22.5}$ during containerless electrostatic levitation processing

Y. J. Kim, R. Busch, and W. L. Johnson
W. M. Keck Laboratory of Engineering Materials, 138-78, California Institute of Technology, Pasadena, California 91125

A. J. Rulison and W. K. Rhim
Jet Propulsion Laboratory, California Institute of Technology, 4800 Oak Grove Drive, Pasadena, California 91109

(Received 13 June 1994; accepted for publication 23 August 1994)

Various sample sizes of $Zr_{41.2}Ti_{13.8}Cu_{12.5}Ni_{10.0}Be_{22.5}$ with masses up to 80 mg were undercooled below T_g (the glass transition temperature) while electrostatically levitated. The final solidification product of the sample was determined by x-ray diffraction to have an amorphous phase. Differential scanning calorimetry was used to confirm the absence of crystallinity in the processes sample. The amorphous phase could be formed only after heating the samples above the melting temperature for extended periods of time in order to break down and dissolve oxides or other contaminants which would otherwise initiate heterogeneous nucleation of crystals. Noncontact pyrometry was used to monitor the sample temperature throughout processing. The critical cooling rate required to avoid crystallization during solidification of the $Zr_{41.2}Ti_{13.8}Cu_{12.5}Ni_{10.0}Be_{22.5}$ alloy fell between 0.9 and 1.2 K/s. © *1994 American Institute of Physics.*

Extensive effort has been devoted to the preparation and characterization of metallic glass alloys.[1] Conventional rapid quenching techniques such as melting spinning, splat quenching, and liquid atomization have been employed to achieve the high undercooling required for glass formation by bypassing heterogeneous nucleation via rapid cooling at 10^3–10^6 K/s. Modest cooling rates of 10^3 K/s or less have been applied to attain deep undercoolings in many binary and ternary alloys such as Pd-Si,[2] Pd-Cu-Si,[3] Au-Pb-Sb,[4] and Pd-Ni-P.[3,5] Very slow cooling rates (0.3 K/s or less) have resulted in sufficiently large undercooling to form glassy Te-Cu alloys in the form of a fine droplet emulsion.[6] To achieve a deeply undercooled liquid state, high-temperature high-vacuum electrostatic levitation[7] has been developed as a containerless process which eliminates the need for a melt containment vessel that often initiates heterogeneous nucleation. Recently, the undercooled melt of a Zr-Ti-Cu-Ni-Be alloy has been found to exhibit extremely high thermal stability.[8] Containerless electrostatic levitation processing was applied to the present investigation to further study the undercooling behavior of the liquid alloy. Information obtained from the present analysis has been coupled with the results from an earlier study of the glass forming ability of this alloy to provide a clearer understanding of the necessary conditions for glass formation (e.g., critical cooling rate) as well as proper thermal treatment of the melt required to suppress heterogeneous nucleation of crystals.

Alloy ingots with the nominal composition $Zr_{41.2}Ti_{13.8}Cu_{12.5}Ni_{10.0}Be_{22.5}$ were prepared from a mixture of elements of purity ranging from 99.5% to 99.9% by induction melting on a water cooled silver boat under a Ti-gettered argon gas atmosphere. Prior to processing, the high-temperature high-vacuum electrostatic levitator (HTHVESL) was evacuated to an ultimate vacuum of 6.7×10^{-3} mPa. Sample heating was provided by a 1 kW UV-rich high pressure xenon arc lamp (ILC, model LX 1000CF). During the melting and solidification process, the sample temperature was measured using an E^2T pyrometer (model 7000ET-1HR) coupled to a readout unit (model E^2T-B) with a nominal sensitivity range of 588–1923 K. The emissivity setting was held constant throughout the experiments and initially set such that the pyrometer read a known eutectic temperature (in this particular alloy, $T_{\text{eutectic}}=937$ K).[8] As long as the sample remains liquid, the error introduced into the temperature measurement as a result of varying sample emissivity is estimated from the Haagen–Rubens emissivity relation to be less than 2% over the measured range.[9] The processed samples were analyzed with x-ray diffraction (XRD) using an Inel position sensitive detector with Co Kα radiation ($\lambda=0.1790$ nm). A Perkin–Elmer DSC 4 scanning calorimeter interfaced to a personal computer for data processing and analysis was used for thermal analysis.

An example of the undercooling behavior observed during solidification is shown in Fig. 1 for a 13.5 mg sample of $Zr_{41.2}Ti_{13.8}Cu_{12.5}Ni_{10.0}Be_{22.5}$. The appearance of recalescence due to crystallization during cooling is indicated in cooling curves A and B. Due to the high vacuum condition during processing, the cooling was purely radiative and was achieved by simply blocking the heating source. Cooling curve A, obtained from the fresh sample, shows that the crystallization is initiated at approximately 853 K. After the first melting and cooling cycle was completed, the same sample was remelted and maintained in the liquid state at 1173 K for about 15 min. Subsequent radiative cooling indicated a crystallization temperature of about 833 K. The same sample was then remelted and maintained at 1173 K for 1 h. The sample was found to solidify without any recalescence during radiative cooling as shown in cooling curve C in Fig. 1.

An XRD pattern of the sample obtained following cooling curve C in Fig. 1 shows only the broad diffraction maxima typical of an amorphous alloy as shown in Fig. 2. Due to the difficulties of XRD analysis on the spherical

 0003-6951/94/65(17)/2136/3/$6.00

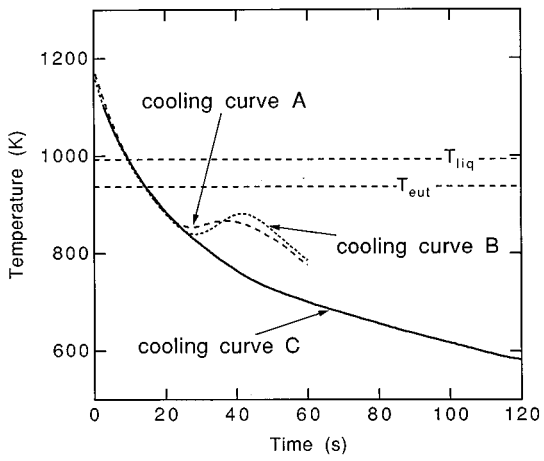

FIG. 1. Temperature profiles for radiative cooling of a $Zr_{41.2}Ti_{13.8}Cu_{12.5}Ni_{10.0}Be_{22.5}$ alloy sample (13.5 mg): curve A is from the first cooling of a fresh sample, curve B is from the second cooling after remelting of the sample for a duration of 15 min, and curve C is from the third cooling (after remelting for 1 h) indicating the liquid is undercooled to the T_g regime without crystallization.

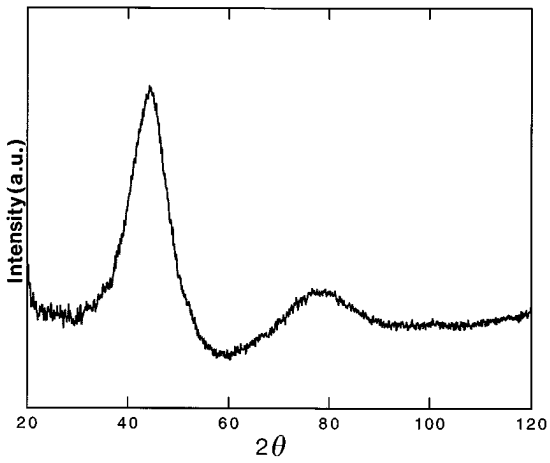

FIG. 2. XRD pattern (Co $K\alpha$ radiation) of the $Zr_{41.2}Ti_{13.8}Cu_{12.5}Ni_{10.0}Be_{22.5}$ alloy sample processed containerlessly in the HTHVESL levitator.

sample, the processed sample was deformed to a thin disk shape using a high pressure die with around 2 GPa pressure. No evidence of crystallinity was observed by XRD following deformation to a thin disk. To further confirm the amorphous state of this sample, differential scanning calorimetry (DSC) was carried out. Figure 3 shows a DSC thermogram of the same sample, which exhibits the onset of a glass transition at 621 K using a 0.67 K/s heating rate. This value is comparable (about 7 K lower) to the T_g of an amorphous reference sample that was prepared by water quenching in a silica tube.[8] The difference may be due to the much slower cooling rate obtained by containerless processing (i.e., radiative cooling at a rate of about 10 K/s) resulting in a more relaxed amorphous state with a lower T_g than that from water quenching which provides a cooling rate of the order of 100 K/s.[13] A total specific heat increase through the glass transition of 21.3 J mol^{-1} K^{-1} in the containerlessly processed sample equals the value obtained from the amorphous reference sample within the experimental error of 2%. In addition, both alloys show identical crystallization behavior (with the same amounts of heat release in the different crystallization peaks). Thus, it can be concluded that a fully amorphous alloy was obtained by cooling in the HTHVESL. This implies that the various catalytic nucleants such as oxide particles or other foreign debris which initiate nucleation were gradually dissolved into the liquid solution during processing above the melting point. With the elimination of heterogeneous nucleants, the sample undercools below the glass transition temperature, T_g, thus forming a glassy alloy. It should be noted also that the process of solidification was carried out under high vacuum conditions (9.3×10^{-2} mPa) to minimize the deposition of impurities on the surface of the sample.

An optical micrograph of a typical glassy sample is shown in Fig. 4. Exceptional smoothness and no crystallinity were observed at the surface of sample. The surface topology was analyzed using atomic force microscope (AFM) indicating that the surface smoothness was about ±5 nm with the typical variation occurring over micrometer length scales.[10]

Of practical importance is the critical cooling rate for amorphous phase formation. Turnbull used the classical nucleation and growth theory of crystalline phases in an undercooled liquid to analyze the glass forming ability of metallic materials.[11] For kinetic analyses [e.g., construction of time-temperature-transformation (T-T-T) diagrams for the initiation of crystallization], numerical values must be assigned to various thermodynamic and kinetic parameters, such as the driving free energy for crystallization, ΔG_v, the liquid-solid interfacial energy, $\sigma_{1/s}$, and the liquid viscosity, η, in the undercooled region. At present, the magnitude of these parameters are uncertain (especially for highly undercooled liquids) due to limited experimental data. As a result, a kinetic analysis may be expected to provide no more than an approximate, order of magnitude, estimate for the critical cooling rate to bypass crystallization. Using unique experi-

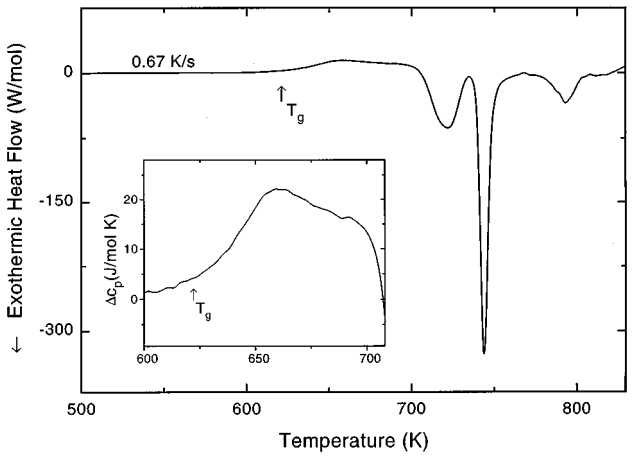

FIG. 3. DSC thermogram (heating rate of 0.67 K/s) of the $Zr_{41.2}Ti_{13.8}Cu_{12.5}Ni_{10.0}Be_{22.5}$ alloy sample processed containerlessly in the HTHVESL. The insert shows the endothermic jump in the signal due to the specific heat increase when the alloy passes the glass transition.

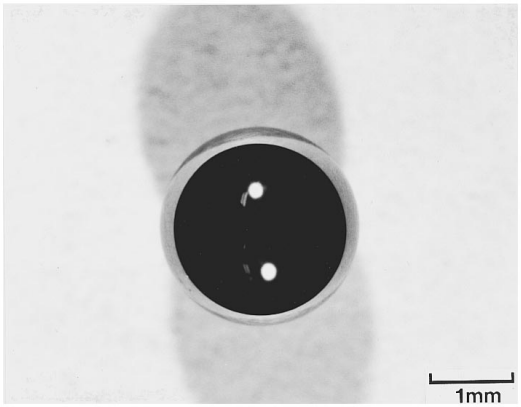

FIG. 4. Optical micrograph of the glassy $Zr_{41.2}Ti_{13.8}Cu_{12.5}Ni_{10.0}Be_{22.5}$ alloy sample processed containerlessly in the HTHVESL.

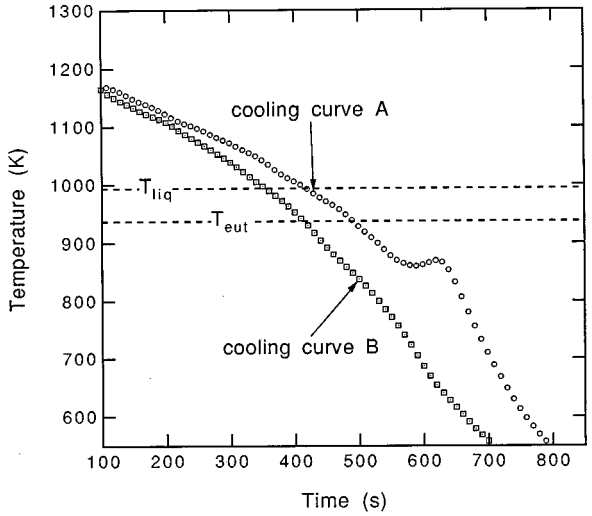

FIG. 5. Temperature profiles obtained at two different cooling rates: curve A is for cooling rate of 0.9 K/s and curve B is for 1.2 K/s.

mental capabilities of HTHVESL at JPL (i.e., sampling heating, cooling, and levitation are decoupled), it was possible to measure the critical cooling rate to bypass crystallization by directly varying the cooling rate. Figure 5 shows the cooling curves obtained at two different cooling rates for a 42.4 mg sample of $Zr_{41.2}Ti_{13.8}Cu_{12.5}Ni_{10.0}Be_{22.5}$. It is interesting to point out that the shape of cooling curves shown in Fig. 5 differs from those in Fig. 1. This is because the cooling curves of Fig. 1 were obtained by completely blocking the heating source of xenon arc lamp (i.e., purely radiative cooling process) while the cooling curves of Fig. 5 were made by gradually reducing the heating power to achieve a slow cooling rate. In Fig. 5, cooling curve A was attained with a cooling rate of 0.9 K/s while cooling curve B with a slightly faster cooling rate of 1.2 K/s. This indicates that a critical cooling rate in excess of 0.9 K/s but less than 1.2 K/s is required to avoid crystallization during solidifica-tion of the $Zr_{41.2}Ti_{13.8}Cu_{12.5}Ni_{10.0}Be_{22.5}$ alloy. It is worthwhile mentioning that due to a sufficiently short internal relaxation time (τ_2) for temperature gradients of small size liquid droplet [i.e., for typical liquid metal drops of 2 mm size in diameter, the internal temperature gradients inside the liquid metal drop are relaxed within less than 0.5 s ($<5\tau_2$)] we can assume that no significant temperature gradients exist across the cross section of the liquid droplet during cooling at the low rates used here.[12] The processed sample was analyzed by XRD and DSC. The results indicated a fully amorphous state after cooling at 1.2 K/s. In addition, taking $T_g=625$ K and $T_{liq}=993$, Fig. 5 shows the total time for cooling without any crystallization (i.e., between T_1 and T_g) to be approximately 5 min. To our knowledge, this is the longest duration cooling cycle reported for an undercooled liquid alloy of scaled-up sample size (mm sizes in diameter).

Based on the present investigation, several comments can be made in regard to containerless processing using HTHVESL as applied to amorphous materials. It has been observed that the application of the HTHVESL technique to the $Zr_{41.2}Ti_{13.8}Cu_{12.5}Ni_{10.0}Be_{22.5}$ alloy has yielded samples sufficiently free of active nucleation catalysts so that configurational freezing (i.e., vitrification) can occur during a slow cooling of relatively scaled-up samples (up to 80 mg). As the duration of holding the molten metal above the liquidus temperature increased, it was possible to ''clean'' the sample and to avoid heterogeneous nucleation resulting from the oxide particles or other contamiants during solidification. Since the thermal history (heating and cooling) is completely decoupled from the levitation of the sample in HTHVESL, and the $Zr_{41.2}Ti_{13.8}Cu_{12.5}Ni_{10.0}Be_{22.5}$ alloy shows exceptionally high thermal stability of undercooled melt, a new opportunity for studying the undercooling and solidification behavior as well as for making experimental measurements of thermophysical properties of the undercooled liquid from T_1 to T_g has become available.[13] For example, in this letter, we have demonstrated direct experimental measurement of the critical cooling rate for glass formation in a newly developed alloy ($Zr_{41.2}Ti_{13.8}Cu_{12.5}Ni_{10.0}Be_{22.5}$) by applying the containerless HTHVESL processing technique.

The authors gratefully acknowledge the support of the National Aeronautics and Space Administration (Grant No. NAG8-954) and the Humboldt Foundation via the Feodor Lynen Program. This work was carried out at the JPL, California Institute of Technology, under contract with the National Aeronautic and Space Administration.

[1] W. L. Johnson, Prog. Mater. Sci. **30**, 81 (1981).
[2] A. J. Drehman and D. Turnbull, Scripta Met. **15**, 543 (1981).
[3] H. S. Chen, Acta Metall. **22**, 1505 (1974).
[4] M. C. Lee, J. M. Kendall, and W. L. Johnson, Appl. Phys. Lett. **40**, 382 (1982).
[5] A. J. Drehman and A. L. Greer, Acta. Metall. **32**, 323 (1984).
[6] J. H. Perepezko and J. S. Smith, J. Non-Cryst. Solids **44**, 65 (1981).
[7] W. K. Rhim, S. K. Chung, D. Barber, K. F. Man, G. Gutt, A. Rulison, and R. E. Spjut, Rev. Sci. Instrum. **64**, 2961 (1993).
[8] A. Peker and W. L. Johnson, Appl. Phys. Lett. **63,** 2342 (1993).
[9] R. Siegel and J. R. Howell, in *Thermal Radiation Heat Transfer,* 2nd ed. (Hemisphere, New York, 1981).
[10] Y. J. Kim, L. M. Madrid, and W. J. Johnson (unpublished).
[11] D. Turnbull and M. H. Cohen, in *Modern Aspect of the Vitreous State,* edited by J. D. Mackenzie (Butterworths, London, 1960).
[12] H. J. Fecht and W. L. Johnson, Rev. Sci. Instrum. **62**, 1299 (1991).
[13] Y. J. Kim, A. J. Rulison, R. Busch, W. K. Rhim, and W. L. Johnson (unpublished).